

Van Goethem, A., Reimer, A., Speckmann, B. & Wood, J. (2014). Stenomaps: Shorthand for shapes. *IEEE Transactions on Visualization and Computer Graphics*, 20(12), pp. 2053-2062. doi: 10.1109/TVCG.2014.2346274



**CITY UNIVERSITY  
LONDON**

[City Research Online](#)

**Original citation:** Van Goethem, A., Reimer, A., Speckmann, B. & Wood, J. (2014). Stenomaps: Shorthand for shapes. *IEEE Transactions on Visualization and Computer Graphics*, 20(12), pp. 2053-2062. doi: 10.1109/TVCG.2014.2346274

**Permanent City Research Online URL:** <http://openaccess.city.ac.uk/14151/>

### **Copyright & reuse**

City University London has developed City Research Online so that its users may access the research outputs of City University London's staff. Copyright © and Moral Rights for this paper are retained by the individual author(s) and/ or other copyright holders. All material in City Research Online is checked for eligibility for copyright before being made available in the live archive. URLs from City Research Online may be freely distributed and linked to from other web pages.

### **Versions of research**

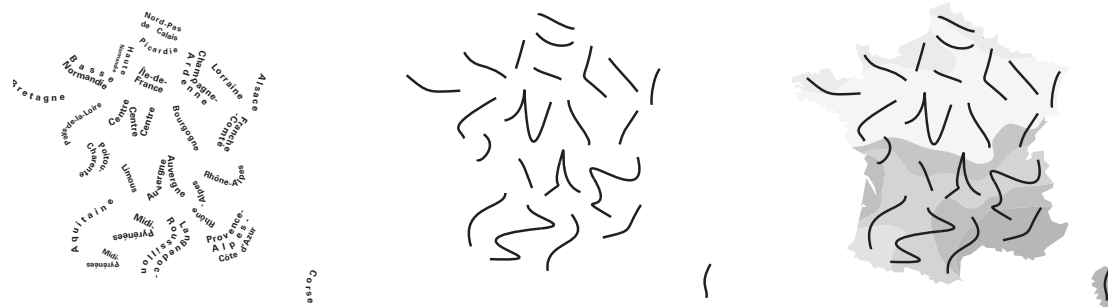
The version in City Research Online may differ from the final published version. Users are advised to check the Permanent City Research Online URL above for the status of the paper.

### **Enquiries**

If you have any enquiries about any aspect of City Research Online, or if you wish to make contact with the author(s) of this paper, please email the team at [publications@city.ac.uk](mailto:publications@city.ac.uk).

# Stenomaps: Shorthand for shapes

Arthur van Goethem, Andreas Reimer, Bettina Speckmann, and Jo Wood



**Abstract**— We address some of the challenges in representing spatial data with a novel form of geometric abstraction – the stenomap. The stenomap comprises a series of smoothly curving linear glyphs that each represent both the boundary and the area of a polygon. We present an efficient algorithm to automatically generate these open,  $C^1$ -continuous splines from a set of input polygons. Feature points of the input polygons are detected using the medial axis to maintain important shape properties. We use dynamic programming to compute a planar non-intersecting spline representing each polygon’s base shape. The results are stylised glyphs whose appearance may be parameterised and that offer new possibilities in the ‘cartographic design space’. We compare our glyphs with existing forms of geometric schematisation and discuss their relative merits and shortcomings. We describe several use cases including the depiction of uncertain model data in the form of hurricane track forecasting; minimal ink thematic mapping; and the depiction of continuous statistical data.

**Index Terms**—Schematisation, Maps, Algorithm, Design

## 1 INTRODUCTION

Generalisation and abstraction are fundamental processes in the construction of cartographic views of data. These can range from straightforward geometric simplification processes that attempt to reduce data volumes without significantly affecting visual appearance to more complex abstractions where referents are more radically transformed into their symbolic representations. The need for higher levels of abstraction may be greater when combined with thematic and other data in an information visualization context with its demand for graphical space and distinct visual variables. Schematisations that preserve topological relationships at the expense of geometric fidelity or cartograms that generate data-centric reprojections of space add to a range of design options available for those wishing to visualize geospatial data. This paper offers a further extension of that design space by providing a new method of transforming two-dimensional polygonal representations into smoothly curving one-dimensional linear features or *glyphs*. This form of extreme geometric abstraction we term the *stenomap*, from the Greek *stenos* meaning ‘narrow’ and a direct analogy with stenography – the transformation of letter form into shorthand symbols. The approach is inspired in part by some of the work

of the 20th century cubist and abstract expressionist artists, including Picasso and Pollock, who explored radical transformations of the depiction of form that were still able to capture something of its essence.

We provide several arguments for considering area-to-line transformations. Fig. 1 displays an ordered sequence of transformations of a polygon increasing in their abstraction. While generalising polygon boundaries is common (Fig. 1(b)), and often valuable, it is constrained by the topological arrangement of adjacent polygonal units along common boundaries. Transformation to a zero-dimensional point feature (Fig. 1(e)) frees up graphical space, however, topological relationships and most geographic context is lost in the process. Transformation to a linear representation offers the opportunity to free up graphical space while maintaining a sense of the form and arrangement of the original feature. Area-to-line transformation is most commonly achieved via medial axis generation (Fig. 1(c)), but while useful as an intermediate step for shape characterisation it has limited cartographic value and may be confused with genuine linear features such as river or road networks. The more smoothly curved stenomap glyphs (Fig. 1(d)) capture something of the form of the polygon boundary while being independent of adjacent polygon geometry and freeing up graphical space for other representations. We describe how stenomaps may be created algorithmically and explore the potential for such representations to open up the design space for the depiction of uncertainty, in thematic mapping and interaction with other visual variables.

**Organization.** We first discuss the design choices for the glyphs used in stenomaps (Section 2). Then we give an efficient algorithm to automatically generate these glyphs from a polygon through medial axis detection (Section 3 and 4). We propose a scoring function which encourages the one-dimensional curve to describe both the boundary and area implied by the polygon. There are different possibilities for the

- Arthur van Goethem and Bettina Speckmann are with TU Eindhoven. E-mail: [a.i.v.goethem|b.speckmann]@tue.nl
- Andreas Reimer is with Universität Heidelberg. E-mail: andreas.reimer@geog.uni-heidelberg.de
- Jo Wood is with City University London. E-mail: j.d.wood@city.ac.uk

Manuscript received 31 March 2013; accepted 1 August 2013; posted online 13 October 2013; mailed on 4 October 2013.

For information on obtaining reprints of this article, please send e-mail to: tvcg@computer.org.

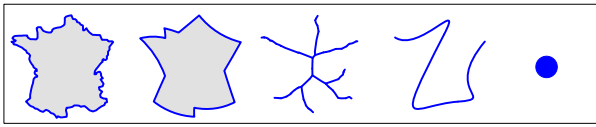


Fig. 1. Increasing the abstraction of France. From left to right: (a) untransformed polygon, (b) curved schematization, (c) pruned medial axis, (d) stenomap glyph, (e) dot.

types of glyphs computed (Section 5) and we describe user-parameters that help explore the possibility-space. We discuss several use-cases (Section 6) to explore the role that stenomap abstraction can have in the depiction of geospatial data. Finally, we conclude with a discussion and possible directions for future work (Section 7).

**Background.** The representation of outlines has received significant attention within the field of cartography. Both straight-line and curve schematisation, as well as simplification, have been well studied. Well known results in cartographic generalisation such as linear simplification (e.g., [14, 20, 39]) maximise the information maintained when reducing the level of detail. Automated cartographic generalisation (for foundational terms and state of the art see, [12, 24, 11]) is driven by intricate knowledge of the target scale or Level of Detail of the map product (e.g., [9]). By contrast, the focus of schematisation is to minimise detail while maximising task-appropriateness of the visualisation [23]. Straight-line schematisations (e.g., [5, 10]) have mainly focussed on orientation-restricted representations. Similarly, curved schematisation (e.g., [17]) has focussed on fixing the type of curve.

Representing shapes using curves has also been considered in other research fields, such as computing tangent-continuous paths for cutting tools (e.g., [15, 19]). Mi *et al.* [27] take an alternative approach, deconstructing a shape into parts to find the required abstraction.

Bézier curves, first described in 1959 [13], are a family of smooth curves described by a set of control points. As the control points define the tangents at the end points of the curve, Bézier curves can be used to create  $C^1$ - or  $C^2$ -continuous splines. Fitting a Bézier spline to a polygonal line can not be optimized in closed form, however iterative algorithms exist (e.g., [26, 32]). Stone and DeRose [36] show how to determine the existence of self-intersections in a cubic Bézier curve.

The medial axis, introduced by Blum [8], is a way to describe the skeleton of a polygon. As the medial axis is not stable under small transformations, various pruning algorithms have been proposed [2, 3, 6, 34]. Only maintaining the parts describing the main features of the polygon gives rise to a more stable version of the medial axis. In computer vision, shock graphs have recently gained considerable attention as this extended structure built on top of the medial axis can be used for automated shape recognition (e.g., [25, 38]).

Space-filling curves are regularly structured curves that fully cover a  $n$ -dimensional space. These curves can be seen as “[mapping] a one-dimensional space onto a higher-dimensional space.” [40]. Recently, the use of space-filling curves to display hierarchical or complex datasets has gained attention (e.g., [1, 37]). In contrast to space-filling curves, our approach focusses on a curve that covers only a part of the area while still sufficiently describing it.

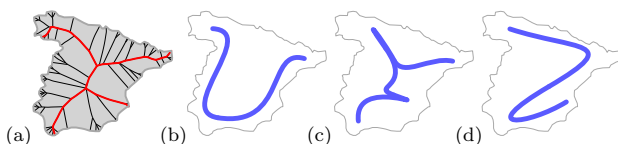


Fig. 2. Representing Spain as a glyph. (a) Polygon and (pruned) medial axis. (b) Border representation. (c) Collapse to medial axis. (d) Trade-off between border and area.

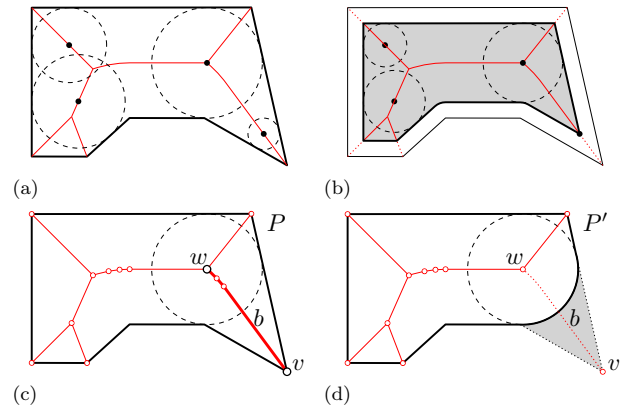


Fig. 3. (a) Four maximally inscribed circles. The center points of all maximally inscribed circles form the medial axis (red). (b) Reducing the radius of all maximally inscribed circles negatively offsets  $P$ . (c) An end-branch  $b$  with parent  $w$  and leaf  $v$ . (d) Area contributed by the end-branch  $b$ .

## 2 DESIGN CHOICES

Reducing a polygon to a line inevitably reduces its expressiveness. Hence, if we desire such an abstraction, careful thought should go into the formation of this line. In this section we discuss the design choices made when developing stenomaps.

**$C^1$ -continuous.** The glyphs we create are (along single strokes)  $C^1$ -continuous. The continuity of the curve gives a hand-drawn appearance stimulating the perceived inexactness of the geometry. Using smooth swipe-like, near casual representations promotes an attention shift to the actual data, further emphasizing the imprecision in the geometry. For a discussion on  $C^x$ -continuity see Section 3.

**Complexity.** All glyphs should be presented using as few curves as possible. The curves should sufficiently describe the polygon at hand, but no excess information should be provided. We target our stenomaps at data not tied to an exact location. As exact geographic information is unimportant and excess information reduces the efficiency of the map, glyphs should have the lowest possible complexity. All attention should be focussed on the main data presented.

**Area and boundary.** Representing a polygon by a linear smooth glyph reduces the expressive power compared to the original two-dimensional polygon. Whereas a polygon implicitly describes both the area and the boundary, this is less clear for an open curve. In the case of elongated polygons both area and boundary representation give overlapping requirements. A curve following the “central axis” suitably describes both. For compact polygons, however, the requirements contradict (see Fig. 2). A partial boundary representation lacks the implied volume of the polygon, whereas a “central axis” is unable to properly represent the shape of the polygon. We note that a trade-off exists between representing the boundary and the area. We require the maximum minimum distance to the curve to be optimized while also sufficiently representing the boundary.

## 3 TECHNICAL PRELIMINARIES

**Medial axis.** The *medial axis transform* was first introduced by Blum [8] and is defined for a polygon  $P$  as the closure of the set of points with two or more closest points located on the boundary of  $P$ . This set is usually simply referred to as the *medial axis* and is a subset of the edges implied by the edge-based Voronoi diagram [4]. The medial axis is a unique description of the shape of  $P$ . Each point on the medial axis is associated with a maximally inscribed circle of  $P$  (see Fig. 3(a)) and the union of all circles fully covers  $P$ . More specifically, there is a one-to-one correspondence between the medial axis including the radii of all maximal inscribing circles and the polygon being represented. This

representation makes it easy to compute offset polygons by changing the radius of all inscribed circles by a fixed constant  $c$  (see Fig. 3(b)). A negative offset (essentially shrinking the polygon) can result in several connected components. Maintaining a minimum circle radius of  $r \geq 0$  prevents such fragmentation.

Our input is a simply connected polygon  $P$ . (Note, though, that our algorithms could easily be extended to polygons with holes.) The medial axis  $M$  of a simply connected polygon is a tree. A *leaf* of  $M$  is a vertex of degree one and is located on the boundary of the input polygon. An *end-branch*  $b$  is a maximal sequence of edges connected via vertices of degree two, where at least one of the two end points is a vertex of degree one (see Fig. 3(c)). An end-branch has two end points, one of which is a leaf, the other is a *parent* (which could simultaneously also be a leaf). An end-branch  $b$  is *pruned* by removing all of the edges and degree one and two vertices of  $b$  from the medial axis. If we reconstruct the polygon belonging to the pruned medial axis we obtain a locally smoothed polygon  $P'$ . The *contributed area* of an end-branch is the area of  $P - P'$  (see Fig. 3(d)). A pruned medial axis can be used for a variety of purposes and hence there exists a significant amount of literature which discusses various pruning measures and methods [2, 6, 29, 33, 34].

**Visibility graphs.** Given a set of points  $S$ , the visibility graph is the union of all edges between any pair of points in  $S$  that can see each other. We use a specific instance of the visibility graph where visibility is defined by the polygon  $P$  and the set  $S$  consists of all vertices of  $P$ . Two points can see each other if the straight-line connection between them is fully contained in the interior or the boundary of  $P$ . We use this visibility graph to compute shortest Euclidean paths in  $P$ .

**Bézier splines.** A cubic Bézier curve can be fit “optimally” to a given polygonal line using iterative Newton-Raphson approximation [32]. Similarly, with the help of *dynamic programming*, a series of cubic Bézier curves can be fit optimally to a polygonal line or a polygon [17].

Splines (the concatenations of Bézier curves) can have different degrees of continuity. A spline is  $C^x$ -continuous if the derivative of degree  $x$  of the spline exists and is a continuous function. When a Bézier spline is  $C^1$ -continuous (smooth), the control points of consecutive curves line up (see Fig. 4(a)). Consequently, fitting curves to different parts of the polygonal line is no longer independent and, therefore, dynamic programming can not guarantee an optimal solution. If we reduce the allowed solution space, by fixing the required tangents at all vertices, the fitting of different curves is independent once more. We require the tangents at each vertex to be perpendicular to the bisector (see Fig. 4(b)). The start- and end-vertex have no well defined tangents, but no continuity is required here either. While fixing tangents beforehand is not required to compute a smooth spline, if tangents are not fixed, computing an *optimal* series of curves is hard.

#### 4 ALGORITHM

We describe an algorithm to compute a linear,  $C^1$ -continuous glyph  $G$  representing a simple input polygon  $P$ . Depending on the desired design, different types of glyphs can be generated (see Section 5).

Our algorithm consists of four distinct steps. First, we detect feature points that define the characteristic shape of  $P$ . Second, we compute the region in which the glyph should be located. Third, we determine the base shape of the glyph by finding a polygonal line (the *backbone*) that represents the polygon well. The shape of the backbone determines the shape of the final glyph to a large degree. Hence we describe

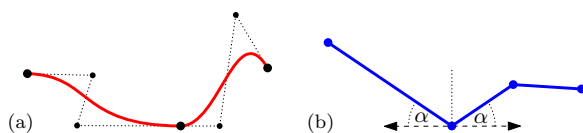


Fig. 4. (a)  $C^1$ -continuous curves have a continuous derivative. The control points of consecutive curves line up. (b) Fixing the required tangent beforehand allows for a dynamic programming solution.

#### Algorithm 1 ComputeGlyph( $P$ )

**Require:**  $P$  is a simple polygon  
**Ensure:**  $G$  is a glyph of  $P$ , strictly positioned inside  $P$

```

{Find feature points}
1: Create the medial axis  $M$  of  $P$ 
2: Prune  $M$  to obtain feature points of  $P$ 
{Obtain glyph region}
3: Trim branches of  $M$ 
4: Simplify  $P$  based on  $M$ 
{Find backbone}
5: Compute all paths between feature points
6: Find the backbone  $B$  visiting all feature points
{Create glyph}
7: Fit a smooth spline to  $B$  to obtain glyph  $G$ 

```

two different approaches which result in radically different backbones. In the final step we fit a cubic Bézier spline to the backbone. Again, there are several possibilities, resulting in different types of glyphs. If the input is planar, our algorithm can be run in parallel on all polygons. See Algorithm 1 for a summary. We explain all steps in detail below.

#### 4.1 Feature points

To maintain the characteristic shape of the input polygon  $P$ , we first detect the main *feature points*. We take a geometric point of view and use the pruned medial axis for feature recognition. Our method is based on the work by Bai and Latecki [2], who use area as a measure to guide the pruning. Area is relatively outlier- and noise-insensitive and is also used as a measure in cartographic simplification [39], making it suitable for our purposes.

The method by Bai and Latecki computes for each end-branch the size of the area that it contributes to  $P$ . By repeatedly pruning the end-branch that contributes the least amount of area to  $P$  the medial axis can be reduced to its main features. The algorithm by Bai and Latecki compares area loss to the previous, already reduced, incarnation of the polygon. As a consequence it may reduce large subtrees by iteratively removing small sections of the area. To prevent important features from being pruned prematurely we maintain the total area that has been pruned in each subtree. We maintain this information in the leaves and parent nodes and update it in amortized constant time when pruning an end-branch. Each edge is pruned only once and we can compute the area lost in  $O(n)$  time, so the total pruning process takes  $O(n^2)$  time. The leaves of the pruned medial axis correspond to the main features.

When displaying a subdivision (e.g., countries in Europe) we typically desire a similar complexity level across the map. To achieve this we admit only pruning steps that remove subtrees of a given maximum size. That is, any single prune action is not allowed to remove a branch representing a subtree larger than a user-specified percentage of the average polygon area in the map. The pruning process stops when this constraint is violated or when only a single path is left.

As discussed in Section 2, elongated polygons and compact polygons require a different level of detail. To facilitate this we introduce an extra factor measuring the compactness of a polygon. Specifically, we use the squared length of the longest path in the medial axis divided by the area of the polygon as a size independent description of compactness (see Fig. 5). Any measure using boundary length instead

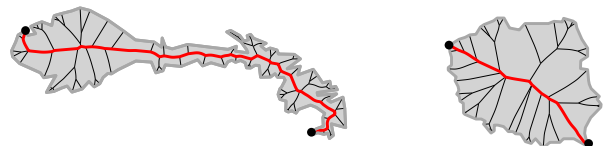


Fig. 5. The ratio between the longest path and the surface area gives a description of the compactness of a polygon. Both polygons are scaled to the same surface area.

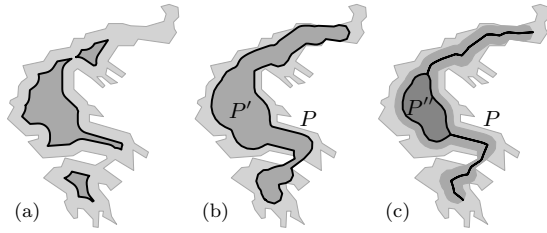


Fig. 6. (a) A regular offset may cause branches to collapse and disconnect the polygon. (b) The offset polygon  $P'$  defines the space for the glyph. (c) The (possibly degenerate) polygon  $P''$  for the backbone.

of the longest path in the medial axis would be more sensitive to local noise. The local area loss accepted in a single prune action is limited by:  $0.25 * \alpha * avgArea * longestPath^2 / polygonArea$ , where  $0 \leq \alpha \leq 1$  is a user-defined parameter.

#### 4.2 Regions

We now compute the region  $P'$  within which the glyph is contained. To make the glyphs clearly distinguishable we require them to be located strictly within the polygon they represent. Where possible a minimum distance to the boundary of the polygon is guaranteed. Using a modified offset operator ensures that a minimum area is maintained within which the glyph can be fit. A regular offset can cause the polygon to become disconnected and may collapse entire branches (see Fig. 6(a)). The modified offset operator uses the radius information stored in the medial axis. We first retract all end-branches of the medial axis by a given percentage (we use 30%). That is, we measure the length of the end-branch and starting at the leaf vertex remove all vertices and edges until the summed length of the removed edges equals 30% of the original end-branch length. If the next edge induces a percentage larger than 30% we shorten that edge and introduce a new leaf vertex.

Now we apply a modified negative offset to the radii stored for the inscribed circles of the medial axis. We reduce the radii of all inscribed circles by a constant – as in a regular offset – unless this forces a radius to drop below a given threshold. In this case we set the radius to the threshold to prevent a collapse of the polygon (inscribed circles with an initial radius smaller than the threshold are simply maintained). Using a strictly positive threshold ensures a single connected polygon, using a threshold of zero can result in a degenerate polygon. The union of all reduced circles uniquely describes the negatively offset polygon. It can be computed in a single traversal of the medial axis. Our offset does not retract end-branches as all circles are maintained.

The region  $P'$  for the glyph is a negatively offset polygon with a strictly positive minimum radius (Fig. 6(b)) to ensure that the curve can turn without intersecting itself or the boundary. Inside the region  $P'$  we compute a second offset polygon  $P''$  (Fig. 6(c)) in which the backbone of the glyph is located (see Section 4.3). When the backbone is turned into a smooth glyph we require some additional space for smoothing and hence the backbone needs to lie in a strictly smaller region than the region of the glyph. Here we do not require a strictly positive minimum radius and, hence,  $P''$  may be degenerate.

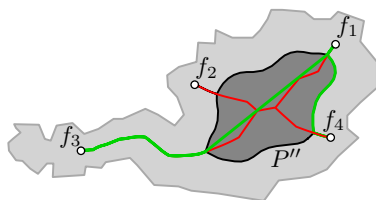


Fig. 7. Consecutive feature points (e.g.,  $f_4, f_1$ ) are connected by a boundary path. Other pairs (e.g.,  $f_1, f_3$ ) are connected by the shortest Euclidean path inside  $P''$ .

#### 4.3 Backbone

A backbone is a planar straight-line graph that visits all feature points and describes the polygon well. We consider two types of backbones: simple paths and trees. Backbones are polygonal representations of the glyphs and are used as base shape for the final glyphs (see Section 5).

**Path-backbone.** Our input is the offset polygon  $P''$  and the feature points cyclically ordered around  $P$  (see Fig. 7). We aim to find a good simple polygonal path visiting all feature points which stays inside or on the boundary of  $P''$ . To do so we first connect any pair of feature points with a path. This path follows the boundary of  $P''$  if it connects two consecutive feature points. For all other pairs we compute the shortest Euclidean path inside  $P''$  using the visibility graph [4].

As discussed in Section 2 the final glyph, and thus the backbone, should represent both area and boundary of the polygon. We represent this dual requirement by a linear trade-off between the percentage of boundary covered and the maximum distance to the curve from any point in the polygon. Let  $s_{boundary}$  and  $s_{area}$  be the boundary and area score respectively and  $0 \leq \beta \leq 1$  a user-set parameter. The score of the backbone is defined as  $(1.0 - \beta) * s_{boundary} + \beta * s_{area}$ .

The boundary score  $s_{boundary}$  represent the percentage of the boundary of the original polygon that is covered by an offset of the backbone. Similarly, the area-score  $s_{area}$  is the maximum minimum distance to the backbone as a percentage of the maximum minimum distance to the polygon boundary (see Fig. 8). As an approximation of the maximum minimum distance we take the maximum minimum distance of any point on the medial axis to the backbone.

Given the computed paths between any pair of feature points and the described weighing scheme, we find the optimal, simple path visiting all feature points. Finding such a path is NP-hard, but as the number of feature points is very small we can use a brute-force approach.

As the backbone is computed using a scoring function we can introduce additional factors to influence the result. For example, our framework implements a penalty function to prevent duplicating parts of the path as well as a sea- or map-border preference. Ensuring the boundary of a map is covered may be preferential if the shape of the subdivision is familiar, but separate polygons are less recognizable. All the figures presented in this paper were, however, created without the use of these additional parameters.

**Tree-backbone.** Path-based glyphs achieve a high level of abstraction. Sometimes a more complex structure may be desirable that better captures the shape and the area of the polygon. We also consider backbones based on trees. Tree-backbones are computed directly from the offset polygon  $P'$ . We turn the boundary of  $P'$  into an undirected graph and detect cycles using depth-first search. Cycles are opened by disconnecting and shortening one of the edges in a cycle.

#### 4.4 Glyphs

The backbone is a concise and abstract representation of the input polygon. In the final step we polish the appearance of the backbone using smooth,  $C^1$ -continuous curves. As the essential shape is already determined by the backbone there is a large degree of artistic freedom in this last step. Several types of glyphs can be created, possibly designed to fit the application at hand. In the next section we describe three possible glyphs that are implemented within our framework.

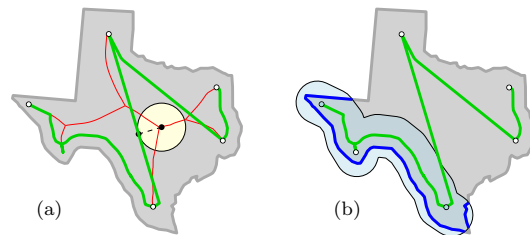


Fig. 8. (a) Maximum minimum distance for any point on the medial axis to the backbone. (b) Boundary covered by a subset of the backbone.

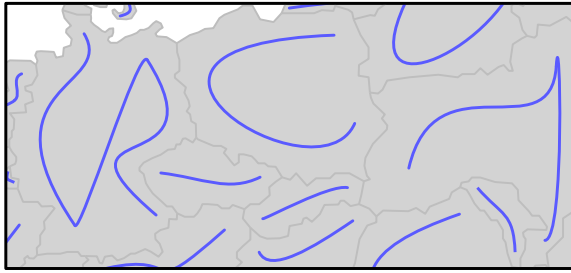


Fig. 9. Example of simple glyphs. Outlines are supplied for reference.

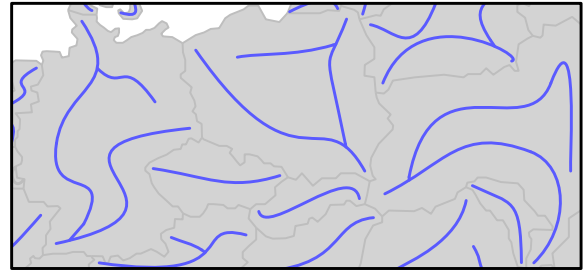


Fig. 11. Example of tree-based glyphs.

## 5 GLYPH TYPES

Different glyphs can be fit onto a backbone and here we discuss three options.

### 5.1 Simple

We fit a simple,  $C^1$ -continuous, cubic Bézier spline to a path-backbone. The simplicity of the design makes this glyph most suitable for cartographic applications. To keep the complexity of the final glyph low, we minimize the number of Bézier curves (see Fig. 9).

The overall spline should use as few curves as possible while staying within a given error-bound  $err_{max}$ . For each single curve  $c$  representing a polygonal line  $p$ , we define its error  $e_c$  as the maximum minimum distance between  $c$  and  $p$ . The error of a set of curves  $C$  is  $\max_{c \in C}(e_c)$ . We use dynamic programming to minimize the number of Bézier curves used to represent the polygonal line while staying within the error-bound [17].

There may be many different splines, using the minimum amount of curves, that stay within the given error-bound of the polygonal line. Therefore, as a secondary objective function for the dynamic program, we compute the average distance  $d_c$  of a curve to the polygonal line. To this end, we compute the average of the squared distances between regularly sampled points along the polygonal line and the curve.

We define the cost  $c$  of a curve as  $1 + d_c / (n * err_{max}^2)$ , where  $n$  is the number of vertices of the polygonal line. As each allowed curve has an error of at most  $err_{max}$ , the average squared distance  $d_c$  is at most  $err_{max}^2$ . The number of curves used to represent the polygonal line can never exceed  $n - 1$ , hence the total cost implied by the fit of the used curves can never exceed one. As a consequence, the result has the minimum number of Bézier curves and has, for all solutions with this number of Bézier curves, the curves with on average the best fit. To prevent curve intersections and self-intersections we set the cost  $c = \infty$  if an intersection occurs.

### 5.2 Locally intersecting

As an alternative to simple,  $C^1$ -continuous cubic Bézier splines we let ourselves be inspired by the work of Picasso (“One-Liners”) [30]. We forgo smooth transitions between consecutive curves and instead cre-

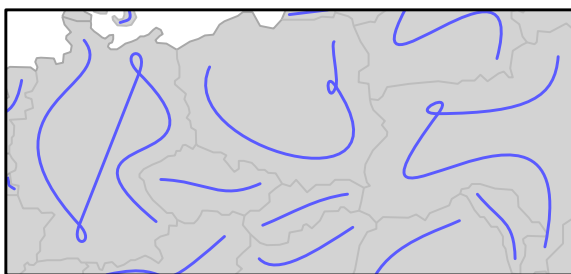


Fig. 10. Example of locally intersecting glyphs.

ate an appearance of smooth behavior by connecting two consecutive Bézier splines with an additional *swirl* (see Fig. 10).

We again use a dynamic program to find the optimal set of fitted Bézier curves. As there is no dependency between consecutive curves, we do not need to fix tangents at the vertices beforehand. For any two consecutive curves connecting at a vertex  $v$ , we compute the distance  $d_{v,p}$  from  $v$  to the polygon  $P$ . We then create an additional cubic Bézier curve (the swirl) whose start- and end-tangents meet up with the previous and next Bézier curve, respectively. To ensure that the swirl is fully located in the polygon the second and third control points of the curve are positioned at a distance  $0.75 * d_{v,p}$  from the first respectively fourth control point. We again disallow intersecting curves.

In some cases swirls may be undesirable. When curves meet at a too shallow or too sharp angle a swirl may look unnatural and a  $C^1$ -continuous connection would be preferred. Let  $C$  and  $D$  be two consecutive curves connected at a vertex  $v$ . Let  $t_C$  and  $t_D$  be the tangents of  $C$  respectively  $D$  at  $v$ . We define  $\alpha$  as the minimal angle between  $t_C$  and  $t_D$ . We only add a swirl if  $\pi/6 \leq \alpha \leq 5\pi/6$ . Otherwise, we force  $C$  and  $D$  to be  $C^1$ -continuous. This creates an interdependency between subproblems and, hence, we cannot claim that the dynamic program computes the optimal solution. In practice, however, the results are quite satisfactory.

### 5.3 Tree-based

The final alternative are glyphs based on tree-backbones. Such glyphs can describe area more concisely, but they are also more complex than glyphs based on path-backbones (see Fig. 11).

Our input is a tree-backbone  $B$ . We say that the leaf of the longest end-branch is the *root* of  $B$ . In case that  $B$  has only two leaves, the root is the top leftmost leaf. Let the *turning angle*  $t_{e,f}$  between two edges  $e, f$  on a path  $p$  be defined as  $\pi - \text{angle}(e, f)$  if  $e$  and  $f$  have a common vertex and 0 otherwise. The turning angle  $t_p$  of a path  $p$  is  $\sum_{e,f \in p} t_{e,f}$ . Let  $P$  be the set of paths of minimum size that cover  $B$ , where all paths  $p \in P$  go strictly down in the tree and  $\sum_{p \in P} t_p$  is minimized. For each path  $p \in P$  we fit a cubic Bézier spline using the edge-based Voronoi diagram to ensure different splines do not intersect [17]. Different splines might not connect at endpoints. We extend splines using a straight line matching the end-tangent to ensure all splines are connected.

## 6 CARTOGRAPHIC APPLICATIONS

We first in Section 6.1 present a formal discussion on the relation of stenomaps to the existing cartographic design space. Section 6.2 to 6.4 explore three use cases for stenomaps.

### 6.1 Stenomaps as thematic maps

The wealth of expressive and effective visualisations in thematic cartography has been subject to numerous efforts of systematisation. The most fundamental of these systematisations is Jacques Bertin’s Semiology of Graphics [7]. Bertin postulates that the effectiveness of any diagram is based on the degree of structural equivalence that can be reached between data and the visual variables. For the case of maps the most powerful variables, the two planar dimensions, are more or

less fixed by geographic coordinates. Any information beyond geometry (thematic *elevation*) must be expressed by encodings using the remaining visual variables known as *retinal variables* or color-pattern variables. The retinal variables are shape, orientation, color, texture, value, size. Each has a maximum in the structural equivalence of the scale level it can express, further limited by the geometric primitive (point, line or area, i.e., *implantation*) it is applied to. The levels of organizations are Association or Disassociation, Selection, Order and Quantity. The Length of a given variable is different for each implantation. Length denotes the number of possible variations that can be used while still allowing selective perception. Bertin discusses each retinal variable and its potential Length thoroughly and with many examples, including special cases and precise instructions on maximizing differentiation. The effects on expressiveness when using multiple retinal variable encodings simultaneously were discussed by [35]. For a discussion of the concept of Disassociation and its effects see [31]. More encyclopedic taxonomies of the actually realised design space were proposed by [16] or [21] for example, which form the baseline of more current works like [22].

The classic space of possible and realised cartographic visualisations [16, 22] divides the topological structure into discrete and continuous phenomena, further subdividing the discrete phenomena into points, lines and areas. Hence, discrete geographic areas can be expressed only by some form of polygonal subdivision. Stenomaps break that contention and show that it is possible to represent discrete areas with cartographic lines. We observe three major changes:

- I boundary lines vanish
- II area fills vanish
- III implantation change from area to line for discrete area objects from the basemap

These changes reduce the visual complexity of the map by reducing the number of control points [23] as well as the amount of “ink” used [7]. Furthermore, change I has the following immediate effects:

- actual locations of boundaries become fuzzy, limiting the accuracy of placement and the ability to conduct measurements in the plane
- adjacency topology becomes fuzzy

- empty bands of expected width  $2 \cdot \epsilon$  become available around discrete areas. Due to isthmuses (see Fig. 6) the theoretical lower bound for width is  $2 \cdot width_{min}^{polygon}$ , i.e. twice the minimal discernable width of polygons, =  $0.6mm$  for b/w and =  $0.8mm$  for color depictions [18].

Effects of change II are:

- maximum selective length for each retinal variable, except shape and orientation is reduced by 1 each. This decreases the degrees of freedom for choosing retinal variables by 4. The reason for this effect can be interpreted as a function of the drawing space real estates that color, texture, value and size need to work at full efficiency.
- maximum selective length for orientation is raised from 0 to 2, as the area implantation does not allow selective variation of orientation at all.
- The net change in degrees of freedom for variation of retinal variables for selective perception is thus  $-2$ .
- figure-ground separation is amplified over the whole map [7]

As the three implantations are highly selective themselves, change III frees up the area implantation for some other feature type to be added but lessens the degree of freedom for other phenomena to be depicted with cartographic lines. The gain of whitespace due to both I and II drastically increases the potential to place further map elements in a high-contrast environment. This decreases visual interaction by simultaneous contrast and color mixing effects. Color can be chosen individually for different implantations. The map in Fig. 12(left) makes use of that effect to display multiple set memberships while having full access to the color space for the point symbols and quantitative data. We can conclude that in cases where the negative consequences of the implantation change *Area*  $\rightarrow$  *Line* such as fuzzy boundaries and adjacencies are not crucial, stenomaps could be used just as well as other maps types like choropleth maps. In cases where displaying sharp administrative boundaries is detrimental to the intended message, stenomaps offer a new cartographic arrangement with improved figure-ground separation, lower complexity, an additional layer-slot for area depictions and a band of white space around the glyphs.

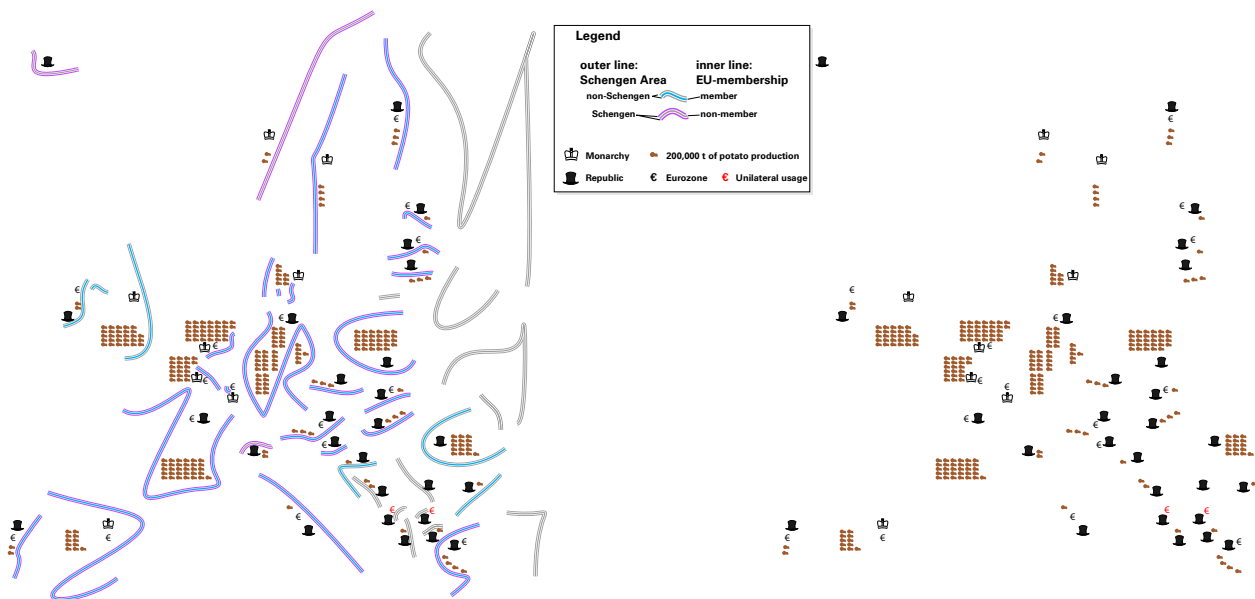


Fig. 12. Potato production, monarchies, the Eurozone and the Schengen accords in the European Union, with and without glyphs.

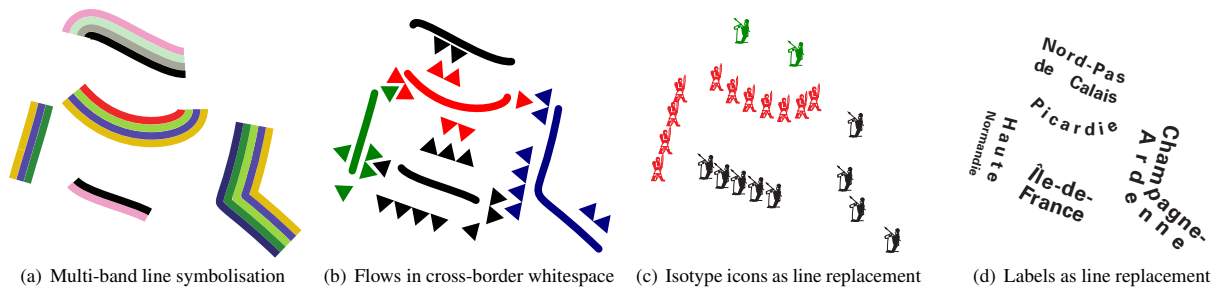


Fig. 13. Design choices for stenomaps.

## 6.2 Use Case: Variations on Glyphs as cartographic lines

In this section, we examine the design possibilities for visual variation of glyphs as cartographic lines. On a fundamental level, glyphs inherit the basic and combinatorial traits of the line implantation, a formal discussion of which we forgo. As visual shorthand for discrete area objects, i.e. in application in a stenomap, we provide some further exploration of design possibilities. Stenomaps do not assume the existence of a separate base map layer. Succinctly, the usual constraints stemming from the base map that line features are limited by, do not apply. This allows a much higher degree of variation in pattern and width of the line features. One example is to create multi-band representations such as Fig. 13(a). Here, multi-set membership and even configurations of set-membership are displayed by colored repetitions of the basic glyphs. Though there are natural limits, these are less strict than in regular maps, due to the white space gained by the area-boundary collapse. Special care must be taken not to vary the width of the glyphs too much, lest the perception as an areal subdivision be dissolved. The same care must be taken regarding brightness (value) differences. Fig. 12(left) makes use of the variation of pattern as well as color. Specifically, the effect of vibration is used following the parametrisation of [7], not unlike a Moiré-pattern, to highlight the Schengen-participants (signatories to a cross-border migration treaty) who are also EU-members. Note that the lower contrast pairings do not produce the same effect. Such use of vibration is generally not advisable for areas and presents another advantage of stenomaps. The glyphs in this figure give a strong sense of location, as can best be seen when making the comparison with the same map solely containing data (see Fig. 12(right)).

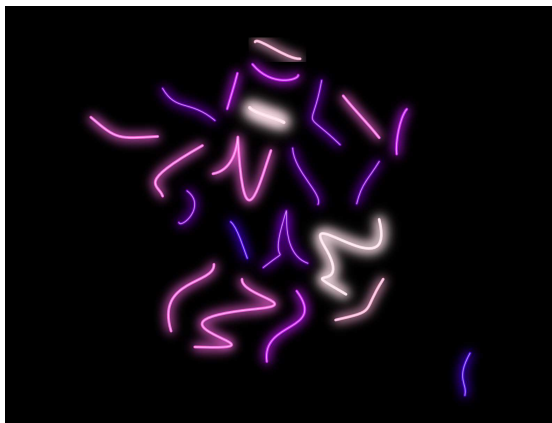


Fig. 14. Energy consumption in the Regions of France 2010. Data source: Electrical Energy Statistics for France 2010, Réseau de transport d'électricité 2011.

While Fig. 12(left) makes use of the space formerly occupied by boundaries by placing point symbols and quantitative information, another possible application is to depict cross-border flows (Fig. 13(b)). This technique is best suited for the case of planar flow graphs and can reintroduce topology information that was made imprecise by the area collapse. The Vienna Method of Pictorial Statistics (e.g., [28]), later known as *Isotype*, was most often used over very sparse base maps or on plain white paper. Stenomaps are a natural environment where Isotype icons can dwell and prosper. They can be applied like regular carto-diagrams as in Fig. 12(left) or even be used to utterly replace glyphs by repetition. The latter technique is limited in cases where the low frequency of icons starts to dissolve the individual glyph, as is exemplified by the green elements in Fig. 13(c).

As has been mentioned, stenomaps abscond from regular base maps and thus have no or very few labels. Either through aesthetic choice or informational necessity, the glyphs can be replaced with the toponyms of the collapsed area features, as shown in Fig. 13(d). Note that the geometric algorithm itself could also be used for proper labeling of areas. The parametrisation must then be adjusted to yield curves of low complexity close to the backbone of the polygon (Fig. 6).

If used as polygon boundaries, cartographic lines can traditionally be used to adumbrate specific area fills. These techniques using hachures for cartographic “hemlines” or repetition for copper-engraving-style waterlining, can be inverted in usage to make glyphs more expressive. Such an inverted hemline as both an adumbration of the area as well as thematic expression was used in Fig. 14. The same effect could be applied by inverted waterlining or hachures, which themselves leave ample amount for further variation. Due to the high contrast environment of stenomaps, said variations are much more poignant and discernible than in regular maps.

## 6.3 Use Case: Spatial uncertainty

As an example of uncertain data we investigate the display of hurricane path predictions (see Fig. 15). Presenting these kinds of two dimensional spatial probability data is critical in many applications. Besides hurricane data, thought may be given to flood predications or dispersion of toxic gas plumes. When presenting spatial data on these types of phenomena (we focus on hurricane paths) often only a small part of the information can be presented on the map. While a lot of information may be known about the probabilities, several problems make their effective display challenging. We discuss two problems: selective perception and the illusion of accuracy.

An efficient map requires that the data being conveyed are presented as clearly as possible. To this end the main data presented should be clearly distinguishable from the additional information displayed, such as geography. One of the aspects that ensures *selective perception* is implantation. Using different implantations can enhance the presentation of the main data, hence, improving the effectiveness of the map. When displaying probability information on regular maps, however, both the geography and the two dimensional probability data are polygons. To allow the information to be clearly separated we would desire different implantations to be used. Obtaining different implan-





Fig. 15. Hurricane Katrina Prediction. Probability that center of storm will pass within 75 statute miles. Datasource: NOAA Hurricane Center.

tations can be achieved by abstracting either of the two data sources. By reducing the geography instead of the probability information we prevent a radical reduction of the information presented, but ensure a high selective perception.

A critical problem when displaying probabilistic data is the *illusion of accuracy*. Maps inherently provide a sense of perceived accuracy which is at odds with the inexactness of the data being provided. For predictions a high level of information should be supplied, but extracting any exact localized conclusions should be prevented. To achieve this often the known data are abstracted, reducing a hurricane path to the single path that is most likely. Abstracting the data, however, results in a radical information loss, reducing the effectiveness of the map to portray the spatial data. The conventional way of addressing this problem of depicting uncertain data is to consider ways of symbolising the uncertainty in the data (hurricane track probabilities in this case), but the stenomap provides an alternative approach. By simplifying the geography instead of the data, we maintain all information present in the data, but prevent users from making possibly erroneous precise inferences. The extreme abstraction of glyphs limits interpretation to generalised regional spatial patterns that reflect the uncertainty in the data. More precise inferences of location are not possible as area and state borders are not exactly described.

#### 6.4 Use Case: Cross-boundary phenomena

Many phenomena are collected and aggregated based on administrative subdivisions that are current at the time of collection. When the data are strongly correlated to these subdivisions or when only a local investigation of the data is required, the inclusion of boundaries helps to emphasize the locality of the portrayed information. Geographical phenomena, however, are often not tied to constructed political subdivisions and require a broader scope for analysis of the phenomena. This is most notably the case for continuous data such as statistical surfaces or data from the realm of geosciences such as climate data.



Fig. 17. Solar potential in Europe for horizontally placed PV-modules. Data source: PVGIS 2012.

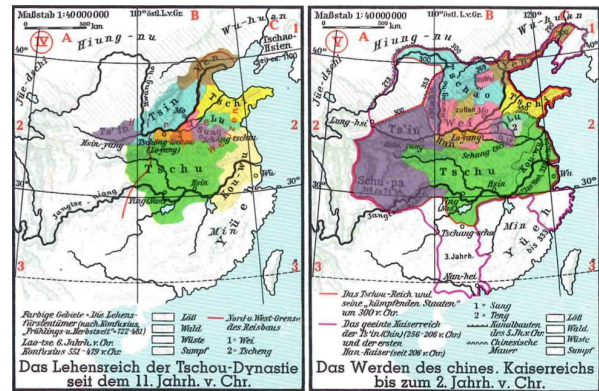


Fig. 16. Example for river line symbols being used as main locational aid. Source: Grosser Atlas zur Weltgeschichte, 1991.

Placing boundaries on top of these kinds of cross-boundary phenomena has long been recognized as unhelpful in many cases:

In the smallest scales, one often just uses a strongly generalised hydrographic network along with the coastlines [as a base map]. – E. Imhof, 1972

The addition of rivers to the map allows for a sense of location even when boundaries are not present. As shown in Fig. 16, sparse base maps with just a strongly generalised line network can be very effective for comparison purposes. The rivers presented fulfill the task normally covered by the boundaries in a map, giving a sense of location that is static across different maps and helps to locate items within the map. The importance of such additional features is most clearly presented by Fig. 17(c). Though the lack of any boundaries ensures that the continuity of the phenomena is emphasized, locating countries on the inside of the subdivision (e.g., Hungary) is hard.

While the introduction of river networks is helpful to give a sense of location on a map, in some cases this information may not be available or desired. Using boundary information instead, however, introduces several problems (see Fig. 17(a)). Closing off areas reduces the perceived continuity of the phenomena as polygons inherently give a stronger sense of positioning of the data. This effect is even further amplified as colors are visually interpreted as more uniform within each polygon. Stenomaps introduce a new, less intrusive way to give a reference to location (see Fig. 17(b)) without implying discrete changes at boundaries. By removing the need to close off areas, the continuity of the described phenomena is better maintained. The inexactness of glyphs ensures that no exact location can be matched with the data. Nevertheless, similar to river networks, glyphs instill a sense of location allowing for comparisons between maps.

## 7 DISCUSSION AND FUTURE WORK

**Evaluation.** The use of linear features to represent polygons is an intriguing new concept that gives rise to stenomaps. We presented an algorithm for the automated construction of stenomaps and discussed a variety of use cases. The results are convincing and visually pleasing. It is, however, unclear how effective stenomaps are. To gauge the usability of stenomaps user studies should be performed in future work. A first step could be to test the recognizability. It should be tested if the proposed glyphs maintain sufficient information for users familiar with the input. After recognizability, task appropriateness should be tested for the different use cases. This will be harder to measure as the glyphs are dissimilar from existing techniques, thereby risking a bias towards more familiar methods. However, task-based evaluation, such as estimation of hurricane damage probabilities over space could provide a useful means of comparison with conventional techniques. Testing the usability of this new method would give a better insight in the strengths and weaknesses of the method; possibly spurring further development.

**Methodology.** The generation of glyphs can be steered using two different parameters. First, by changing the level of pruning of the medial axis the complexity of the final glyph can be determined. Second, the computed backbone can be set to better represent area or boundary. The interplay of these variables allows for a large range of design options (see Fig. 18). These options allow map designers more choice over the shape of the glyphs. However, the question arises if it is possible to define a base setting appropriate for most maps. This is already partially the case as differently shaped polygons within one map are presented using the same settings. Preliminary experiments, however, show that a standard base setting across different maps is unlikely as different maps require different levels of detail. Subdivisions with uniquely shaped polygons require less exact detail than more uniformly shaped subdivisions (e.g., the difference between the states of the USA and the countries of Europe).

The medial axis as a shape-descriptor is very suitable for the creation of glyphs. It allows both feature points to be detected and an efficient computation of the available space. The medial axis is a representation of the polygon space, however it is not necessarily a fair sample. In parts where the inscribed circles are large the medial axis may be far removed from sections of the polygon. Thus, the medial axis may be a false sample when computing the maximum minimum distance to the backbone (Section 4.3). Misrepresenting the area of the polygon can result in visual artifacts as sections of the polygon may not be taken into account. The boundary representation that is part of the scoring function counteracts these effects. Though misrepresentation is unlikely, future work might investigate if other distance measures can give a better representation of the area.

**Glyphs.** Glyph representations allow a significant abstraction from the original input. This level of abstraction is a main feature of the stenomap, but also brings forth new considerations. The representation of polygons through glyphs is very useful when information about a subdivision is shown. The extreme level of abstraction, however, implies that glyphs maintain their meaningfulness only while in context. When less context is present a larger amount of detail should be maintained in the glyphs. Displaying more detail within the glyph, however, reduces the advantage of using glyphs. Another consideration introduced by the extreme abstraction of glyphs is their uniqueness. As glyphs are highly abstracted, similarly shaped polygons may end up with a near similar glyph. While glyphs are distinguishable through their positioning in the subdivision, having uniquely shaped glyphs may be beneficial in some maps where lookup tasks are important. Similar shapes create a visual connection, which might counteract the data being presented. For future work it would be interesting to see if unique glyphs can be guaranteed. Taking similarity into account during the creation of glyphs is likely undesirable when fast computation is essential, since it introduces dependencies between subproblems and inhibits parallel computation.

The minimal information maintained in glyphs is still sufficient to give an inexact description of the input shape. It can be argued that

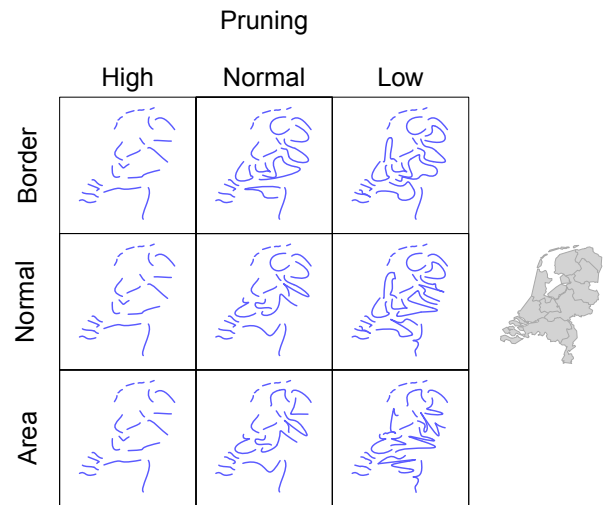


Fig. 18. A sample of the parameter space defined by the user parameters affecting complexity and polygon representation.

the main strength of glyphs is bound by their subconscious relation to the original input shapes. There is a danger that when the user has no knowledge about those shapes, glyphs could lose part of their strength. We would argue, however, that the glyph in itself becomes a representation of the shape that is sufficient for many tasks where precise geometry of polygonal regions is not central. Glyphs supply sufficient information even when the input division may not be well known (e.g., Fig.14).

Through their simplicity glyphs make an interesting case for user interaction. Clearly, glyphs can be used as an additional visualization tool. Glyphs reduce the visual input complexity, which can be beneficial when a high-level overview is required. Their smoothness and simplicity, however, also makes glyphs intriguingly suitable for swipe interaction. Through swipe gestures item selection or map interaction could be achieved. For this use case, unique glyphs would be required.

Stenomaps are very efficient when exact boundaries of a subdivision are not needed but a general representation of the shape is helpful. They also offer several unique graphical variations that are applicable to various common use-cases. But by their intended nature of being a one-dimensional visual shorthand for a two-dimensional object they are still tied to size differences of the input polygons. Succinctly, they share the problems of polygons when directly trying to display quantities by size modification. However, as they are one-dimensional, they conceptually offer the opportunity to address this fundamental limitation of cartography. Thus, future work might explore if it is feasible to ensure that all glyphs have equal length. As glyphs are independent of each other this could, for example, allow for distortion-free cartograms. However, it is unclear whether such an approach would be feasible. First, different sized polygons might coexist in a map (e.g., Luxembourg and Russia). Using too small glyphs would be unsuitable for large polygons, whereas too large glyphs could quickly fill up small polygons. Second, even given equal length, glyph shape still affects the visual saliency. Nevertheless, stenomaps might point the way towards a distortion-free solution of the value-by-area problem.

## ACKNOWLEDGMENTS

Collaboration on this project was started at Dagstuhl seminar 13151 "Drawing graphs and maps with curves". The authors would like to thank Herman Haverkort for inspiring discussions on the subject. A. van Goethem and B. Speckmann are supported by the Netherlands Organisation for Scientific Research (NWO) under project no. 612.001.102 (AvG) and no. 639.023.208 (BS).

## REFERENCES

- [1] D. Auber, C. Huet, A. Lambert, B. Renoust, A. Sallaberry, and A. Saulnier. Gospermap: Using a gosper curve for laying out hierarchical data. *IEEE Transactions on Visualization and Computer Graphics*, 19(11):1820–1832, 2013.
- [2] X. Bai and L. Latecki. Discrete skeleton evolution. In *Energy Minimization Methods in Computer Vision and Pattern Recognition*, pages 362–374. Springer, 2007.
- [3] X. Bai, L. Latecki, and W.-Y. Liu. Skeleton pruning by contour partitioning with discrete curve evolution. *IEEE Transactions on Pattern Analysis and Machine Intelligence*, 29(3):449–462, 2007.
- [4] M. de Berg, O. Cheong, M. van Kreveld, and M. Overmars. *Computational geometry: algorithms and applications*. Springer, 3rd edition, 2008.
- [5] M. de Berg, M. van Kreveld, and S. Schirra. A new approach to subdivision simplification. In *Proceedings of the 12th International Symposium on Computer-Assisted Cartography*, volume 4, pages 79–88, 1995.
- [6] A. Beristain, M. Graña, and A. Gonzalez. A pruning algorithm for stable voronoi skeletons. *Journal of Mathematical Imaging and Vision*, 42(2-3):225–237, 2012.
- [7] J. Bertin. *Graphische Semiologie. Diagramme, Netze, Karten*. Gruyter, 1973.
- [8] H. Blum. A transformation for extracting new descriptors of shape. *Models for the perception of speech and visual form*, 19(5):362–380, 1967.
- [9] C. Brewer and B. Buttenfield. Mastering map scale: balancing workloads using display and geometry change in multi-scale mapping. *Geoinformatica*, 14:221–239, 2010.
- [10] K. Buchin, W. Meulemans, and B. Speckmann. A new method for subdivision simplification with applications to urban-area generalization. In *Proceedings of the 19th ACM SIGSPATIAL GIS*, pages 261–270, 2011.
- [11] D. Burghardt, C. Duchêne, and W. Mackaness, editors. *Abstracting Geographic Information in a Data Rich World - Methodologies and Applications of Map Generalisation*. Springer, 2014.
- [12] B. Buttenfield and R. McMaster, editors. *Map Generalization - Making Rules for Knowledge Representation*. Longman, 1991.
- [13] P. De Casteljau. Outillages méthodes calcul. Technical report, A. Citroën, 1959.
- [14] D. Douglas and T. Peucker. Algorithms for the reduction of the number of points required to represent a digitized line or its caricature. *Cartographica*, 10(2):112–122, 1973.
- [15] R. Drysdale, G. Rote, and A. Sturm. Approximation of an open polygonal curve with a minimum number of circular arcs and biarcs. *Computational Geometry: Theory and Applications*, 41(1-2):31–47, 2008.
- [16] U. Freitag. *Kartographische Konzeptionen - Cartographic Conceptions*, chapter Die Eigenschaften der kartographischen Darstellungsformen, pages 115–132. Freie Universität Berlin, 1992.
- [17] A. van Goethem, W. Meulemans, A. Reimer, H. Haverkort, and B. Speckmann. Topologically Safe Curved Schematization. *The Cartographic Journal*, 50(3):276–285, 2013.
- [18] G. Hake, D. Grünreich, and L. Meng. *Kartographie Visualisierung raumzeitlicher Informationen*. Walter de Gruyter, Berlin, New York, 2002.
- [19] M. Heimlich and M. Held. Biarc approximation, simplification and smoothing of polygonal curves by means of Voronoi-based tolerance bands. *International Journal of Computational Geometry and Applications*, 18(3):221–250, 2008.
- [20] H. Imai and M. Iri. Computational-geometric methods for polygonal approximations of a curve. *Computer Vision, Graphics and Image Processing*, 36(1):31–41, 1986.
- [21] E. Imhof. *Thematische Kartographie*. Walter de Gruyter, 1972.
- [22] M. Kraak and F. Ormeling. *Cartography: Visualization of Spatial Data, Second Edition*. Addison Wesley Longman, subsequent edition, 2003.
- [23] W. Mackaness and A. Reimer. Generalisation in the context of schematised maps. In *Abstracting Geographic Information in a Data Rich World. Methodologies and Applications of Map Generalisation*. Springer, 2014.
- [24] W. A. Mackaness, A. Ruas, and L. T. Sarjakoski, editors. *Generalisation of Geographic Information: Cartographic Modelling and Applications (International Cartographic Association)*. Elsevier Science, 1st e edition, April 2007.
- [25] D. Macrini, S. Dickinson, D. Fleet, and K. Siddiqi. Object categorization using bone graphs. *Computer Vision and Image Understanding*, 115(8):1187–1206, 2011.
- [26] A. Masood and S. Ejaz. An efficient algorithm for robust curve fitting using cubic Bezier curves. In *Advanced Intelligent Computing Theories and Applications*, LNCS 6216, pages 255–262, 2010.
- [27] X. Mi, D. DeCarlo, and M. Stone. Abstraction of 2D shapes in terms of parts. In *Proceedings of the 7th International Symposium on Non-Photorealistic Animation and Rendering*, pages 15–24, 2009.
- [28] O. Neurath. *Gesellschaft und Wirtschaft. Bildstatistisches Elementarwerk*. Bibliographisches Institut Leipzig, 1931.
- [29] R. Ogniewicz and O. Kübler. Hierarchic voronoi skeletons. *Pattern recognition*, 28(3):343–359, 1995.
- [30] P. Picasso and S. Galassi. *Picasso's One-Liners*. Artisan, 1997.
- [31] A. Reimer. Squaring the circle? bivariate colour maps and jacques bertins concept of disassociation. In *International Cartographic Conference*, pages 3–8, 2011.
- [32] P. Schneider. An algorithm for automatically fitting digitized curves. In *Graphic Gems*, pages 612–626. Academic Press Professional, 1990.
- [33] D. Shaked and A. Bruckstein. Pruning medial axes. *Computer Vision and Image Understanding*, 69(2):156–169, 1998.
- [34] W. Shen, X. Bai, R. Hu, H. Wang, and L. Latecki. Skeleton growing and pruning with bending potential ratio. *Pattern Recognition*, 44(2):196–209, 2011.
- [35] E. Spiess. Eigenschaften von kombinationen graphischer variablen. *Grundsatzfragen der Kartographie*, pages 280–293, 1970.
- [36] M. Stone and T. DeRose. A geometric characterization of parametric cubic curves. *ACM Transactions on Graphics*, 8(3):147–163, 1989.
- [37] S. Tak and A. Cockburn. Enhanced spatial stability with hilbert and moore treemaps. *IEEE Transactions on Visualization and Computer Graphics*, 19(1):141–148, 2013.
- [38] N. Trinh and B. Kimia. Skeleton search: Category-specific object recognition and segmentation using a skeletal shape model. *International Journal of Computer Vision*, 94(2):215–240, 2011.
- [39] M. Visvalingam and J. Whyatt. Line generalisation by repeated elimination of points. *Cartographic Journal*, 30(1):46–51, 1993.
- [40] M. Wattenberg. A note on space-filling visualizations and space-filling curves. In *IEEE Symposium on Information Visualization*, pages 181–186. IEEE, 2005.